Chapter 5

Verification – Intercomparison of Solar Radiative Transfer

While chapter 4 dealt with the verification of modeling radiative transfer driven by thermal emission, this chapter examines the implementation of scattering atmospheres illuminated by an external beam source like the sun. The evaluation of solar radiative transfer modeling is based on the intercomparison of SARTre modeling results to those of the full spherical Monte Carlo model McSCIA (Spada et al., 2006), which is introduced in section 5.1.

As described in chapter 3, single scattering of radiation from a beam source and multiple scattering contribution are handled separately in SARTre. The multiple scattering contribution is derived from radiative transfer calculations on the basis of plane-parallel or pseudo-spherical slab geometries, whereas the single scattering contribution is computed accurately in a spherical shell atmosphere. Based on different approaches, single scattering and total scattering contributions are studied individually. Single scattering (SS) results are evaluated in subsection 5.3.1. In subsection 5.3.2 results of the intercomparison of the total scattering (TS) contributions, i.e. the sum of single scattered and multiple scattered (MS) radiation are discussed.

In contrast to modeling of longwave RT, where only a limited section of the atmosphere, e.g. a cloud layer, gives a significant scattering contribution, in shortwave radiative transfer scattering has normally to be taken into account in the whole atmosphere or at least in the troposphere and lower stratosphere. Thus, a broader examination of the limits of the pseudo-spherical assumption is possible.

The setup of this intercomparison, described in detail in section 5.2, is taken from Loughman et al. (2004). A number of viewing geometries for two wavelengths in the ultraviolet (UV) spectral region is studied. As stated in section 3.2, molecular scattering, which is dominating in the UV, is not considered in SARTre. Nevertheless, Rayleigh scattering can be accounted for, when optical properties are provided to SARTre in the manner as particle properties are given (see section 3.3). With single scattering albedo and optical thickness of the atmospheric layers being provided as model input within this intercomparison, no line-by-line calculation of molecular cross sections has been carried out and intercompared here. Furthermore, SARTre had to be slightly adjusted to be able to handle the setup definition. Consistency with the standard model has been checked for a simple setup with only a few layers.

5.1 Models in the Intercomparison

In this section, first the McSCIA model is introduced. A second subsection is dedicated to further models, which are referred to in this chapter. This includes the MCC++ and the LIMBTRAN model, that took part in the intercomparison discussed in Loughman et al. (2004) as well as DISORT and the STORM model, which are used for checking the quasi plane-parallel mode of SARTre.

5.1.1 The McSCIA Model

McSCIA (**M**onte **C**arlo for **SCIA**machy) is a multiple scattering Monte Carlo 3D radiative transfer model (Spada et al., 2006). The algorithm is formulated as a function of Earth radius, such that simulations in both spherical and (quasi) plane-parallel atmospheres may be performed. Refractive bending is neglected. A backward method is used, meaning the path of photons is traced back from the satellite through the atmosphere till the photon is absorbed or escapes to space. The individual event a photon undergoes at a certain time – scattering by air molecules or aerosols, absorption by trace gases, reflection or absorption by the surface – is calculated on the basis of probability density functions.

The model is designed for calculating scalar radiances in the UV-VIS-NIR spectral region. Since thermal emission can generally be ignored in this spectral region, the sun is the only source of light. That means, all photons contributing to the observed radiance have to leave/enter[1] the atmosphere to/from sun direction. To avoid tracing a huge numbers of irrelevant photons, for each photon the probability of leaving the atmosphere towards the sun is calculated. Furthermore, the photons are not allowed to leave the atmosphere after undergoing only a single scattering process. The single scattering contribution is computed separately. Being developed with focus on trace gas observation, two ways of treating absorption have been implemeted in McSCIA. One of them uses the single scattering albedo while the other is based on the equivalence theorem. The latter allows scattering and absorption to be separately taken into account, and absorption may be calculated "off-line" of the scattering solution. Thus, it is possible to re-use the scattering solution in radiance calculations with varied trace gas contents, which may result in eminent reduction of computation time.

The implementation of spherical geometry in McSCIA has been tested against calculations by Adams and Kattawar (1978) and Kattawar and Adams (1978). The verification of the "full 3D" mode has been done in comparison to MCC++ (Postylyakov, 2004) with a setup that had been adapted from a case presented in Loughman et al. (2004), which was related to SOLSE/LORE instruments' viewing geometry. But, all of these test cases had a setup with an absorbing surface for lower boundary.

5.1.2 Further Models

With the setup of the SARTre–McSCIA intercomparison taken from this limb model intercomparison, it is reasonable to consider and compare results of Loughman et al. (2004). This is further supported by the fact, that two of the models intercompared therein are closely linked to SARTre and McSCIA. While the latter has been verified by intercomparing to MCC++, the concept of LIMBTRAN is very similar to SARTre's basic principles.

[1] While in reality photons enter the atmosphere, in backward models like McSCIA they are traced from the observer towards the point, where they virtually leave the atmosphere.

LIMBTRAN

LIMBTRAN may be run in pseudo 3D mode (Griffioen and Oikarinen, 2000), but has been used in Loughman et al. (2004) for calculations of limb radiances in a 1D spherical shell atmosphere, neglecting polarization as well as refraction effects. Like SARTre, LIMBTRAN computes the single scattering contribution accurately in a spherical atmosphere and uses a plane-parallel model for the calculation of the radiation field needed for the multiple scattering source term. These radiation field calculations are carried out by a pseudo-spherical version of a one dimensional finite difference model at a series of points along the line of sight (LOS). Similar to SARTre, it uses Gaussian quadrature for polar angle integrals and Fourier expansion to separate azimuthal dependencies. For computational optimization, Fourier expanded source terms are only evaluated for a selected set of polar angles around horizontal direction and interpolated to required angles later on. The source function integration along the LOS is done using a second order Lagrangian interpolation between grid points to account for the variation of the source function terms along the LOS.

MCC++

MCC++ (Postylyakov, 2004) is a Monte Carlo model, that has been used in the intercomparison of Loughman et al. (2004) as well as to verify the McSCIA model. Besides both being backward models, MCC++ was chosen for the McSCIA verification due to the use of a piecewise constant distribution function of optical properties of the atmosphere. In contrast to the common understanding of the Monte Carlo method, only the multiple scattering contribution is calculated using statistical methods, while single scattering contributions are analytically derived. The statistical accuracy of the MCC++ calculations presented in Loughman et al. (2004) is given by 0.1 %.

DISORT and STORM

DISORT and STORM are used to check the quasi plane-parallel mode of SARTre in subsection 5.3.2. For an overview of DISORT see subsection 3.4, where it is described in its role as plane-parallel solver of the incident radiation field in SARTre. STORM is a plane-parallel vector radiative transfer model that relies on the matrix operator doubling and adding method for the solution of the RT problem (Böttger et al., 2005). It has been used in addition to DISORT to also check against an independent model.

5.2 Intercomparison Setup of Atmosphere and Geometry

The atmospheric and geometric setup is adapted from Loughman et al. (2004), where six full and "approximate" spherical RT models were intercompared with a focus on ozone remote sensing in the UV. Molecular absorption has been restricted to ozone absorption. MODTRAN tropical atmosphere density and ozone profiles were used (Berk et al., 1989) and combined with ozone absorption cross sections from Burrows et al. (1999). In contrast to the original setup, here the atmosphere was taken to be clear of clouds or aerosols, i.e. only Rayleigh scattering by air molecules was assumed. Rayleigh scattering cross sections were taken from Bates (1984) (see also Spada et al., 2006). Atmospheric setup of the intercomparison is defined by resulting layer optical thickness and layer single scattering albedo, which have been provided to the models.

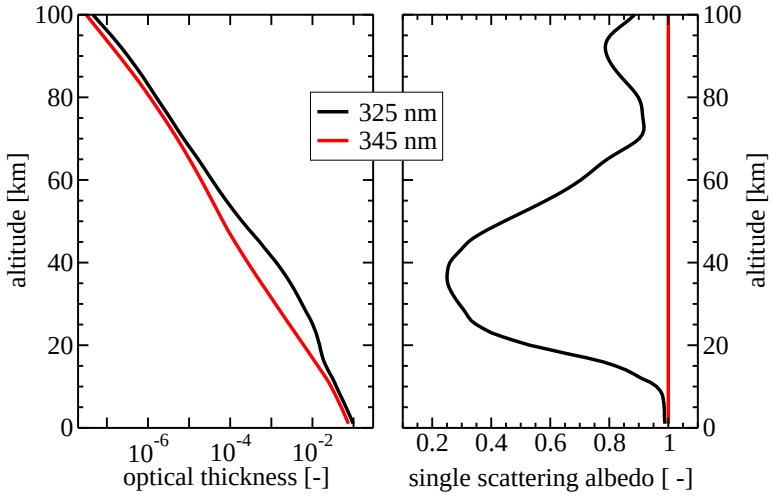

Figure 5.1: *Atmospheric optical properties in solar RT intercomparison: profiles of layer optical thickness (right) and single scattering albedo (left) for $\lambda = 325\,nm$ and $\lambda = 345\,nm$. Scattering phase function is given by Eq. (2.25).*

Atmospheric layers are assumed to be homogeneous, i.e. optical properties have discontinuities at the layer boundaries. The atmosphere, consisting of layers of 1 km physical thickness, is defined between 0 and 100 km (see Fig. 5.1). SARTre and McSCIA modeled radiances have been intercompared at wavelengths $\lambda = 325$ nm and $\lambda = 345$ nm. While $\lambda = 325$ nm is located in the wing of the UV-B ozone band, at $\lambda = 345$ nm the atmosphere is conservative due to negligible ozone absorption. The standard Rayleigh scattering phase function (Eq. (2.25)) is introduced to describe the angular dependency of scattering properties. At both wavelengths, a totally absorbing surface ($r = 0.0$) and a surface, assumed to be a Lambertian reflector with albedo $r = 1.0$, are considered.

Observation geometry varies concerning viewing direction and solar angles. Limb radiances are calculated for tangent altitudes between 10 km and 60 km with intervals of 5 km and a spherical Earth of radius $R = 6371$ km. The set of examined sun geometries, presented in Tab. 5.1, includes a close-to-nadir case and forward, sideward and backward scattering cases for low sun positions.

Solar irradiance is set to unity for all cases. Polarization effects as well as refractive bending are generally neglected.

Table 5.1: *Evaluated sun geometries. All angles are defined at the tangent point of the individual line of sight.*

case n°	1	2-1	2-2	2-3	3-1	3-2	3-3
sun zenith angle (sza)	15°	80°	80°	80°	90°	90°	90°
relative azimuth (az)	90°	20°	90°	160°	20°	90°	160°

5.3 The Intercomparison Cases – Results and Interpretation

In contrast to multiple scattering, single scattering contribution from a beam source is independent of the incident diffuse radiation field. In SARTre, single scattering intensity is derived considering full sphericity of the Earth-atmosphere system. Verification starts with the intercomparison of single scattering limb radiances, which have been shown to account for 45 – 95 % of the total scattering contributions, depending on wavelength and sun geometry (Kaiser et al., 2001). Thus, single scattering calculations provide a benchmark concerning achievable accuracy. Total scattering contributions are compared in the second part. The models are compared on the basis of percentage differences of the calculated intensities with McSCIA modeled radiances used as reference:

$$\Delta I_{\%} \;=\; \frac{I_{\mathrm{SARTre}} - I_{\mathrm{McSCIA}}}{I_{\mathrm{McSCIA}}}. \tag{5.1}$$

With atmospheric conditions defined by single scattering albedo and optical thickness of homogeneous layers, a number of issues in radiative transfer modeling is not addressed. On the one hand this ensures a higher comparability of model results, on the other hand the validity of some customarily used parameterizations and assumptions remain unchecked. In particular, homogeneity of the layers embodies a constant single scattering albedo and a constant density or extinction coefficient of the overall layer. That means optical path lengths may be determined directly and exact by $\tau_s = \tau_z \frac{\Delta s}{\Delta z}$ instead by parameterization according to Eq. (3.9). Furthermore, optical properties within a path segment are constant by definition, i.e. satisfy the linearity assumption to source terms or soure term components (see section 3.1.1). Problems due to non-linearity of single scattering albedo, as occurred for particular layers of the clouds in the terrestrial intercomparison (see 4.6), are circumvented.

Besides providing a general understanding of radiance behavior for different atmospheric conditions and observing geometries, from investigating and intercomparing the single scattering contributions the source integration technique can be confirmed. In addition, limits of the linearity assumption to the geometry dependent parameters of the single scattering source terms are examined. From intercomparison of total scattering radiances, including the contributions from single and multiple scattering, the validity and accuracy of assuming local planarity is evaluated.

5.3.1 Single Scattering Limb Radiances

When only considering solar single scattering, the radiative transfer equation (3.1) reduces to

$$I \;=\; I_{\mathrm{dir}}\,\mathcal{T}_{\mathrm{dir}} \;+\; \int_0^{\infty} J_{\mathrm{SS}}(\tau')\,\mathrm{e}^{-\tau'}\,\mathrm{d}\tau'. \tag{5.2}$$

where $I_{\mathrm{dir}}\,\mathcal{T}_{\mathrm{dir}}$ denotes the transmitted background contribution, with $I_{\mathrm{dir}} \equiv 0$ in non-occultation limb cases, and τ' is the path optical depth along the line of sight. The single scattering source term J_{SS} is given by

$$J_{\mathrm{SS}} \;=\; \frac{\omega_0}{4\pi}\,P(\Theta)\,F_{\odot}\,\mathcal{T}_{\odot}, \tag{5.3}$$

with single scattering albedo ω_0, Rayleigh scattering phase function $P(\Theta)$ given according to Eqs. (2.25) and (2.26), solar irradiance $F_{\odot}$ and transmission $\mathcal{T}_{\odot}$ of the sun light from top of atmosphere (TOA) to the individual scattering point.

Results are shown in Fig. 5.2. In the upper atmosphere limb radiances (see Fig. 5.2(a) and (c)) increase exponentially with decreasing tangent altitude. This occurs for optically thin lines of sight, for which the radiance is proportional to the amount of scatterers along the path. For these cases, limb radiances are further observed to be nearly independent of solar zenith angle, but slightly varying with azimuthal angle due to varying single scattering angle and thus, scattering phase function. Correspondingly, radiances for azimuthal angles of $\mathrm{az} = 20°$ and $\mathrm{az} = 160°$ are equal because of the symmetry of the Rayleigh phase function. When the LOS becomes optically thick, i.e. $\tau \gg 1$, saturation effects appear: limb radiances increase slower (a significant part of the radiation that is scattered into the LOS is scattered out again before reaching the observer) or stagnate (scattering in and out of the path balance each other) or even decrease (scattering into the path is very low, e.g. because sun light is not able to penetrate deeper layers of the atmosphere) with further decreasing tangent altitude. Because of an overall thicker atmosphere at a wavelength of 325 nm (see Fig. 5.1), this happens at a higher tangent altitude (≈ 40 km) than for 345 nm (≈ 30 km).

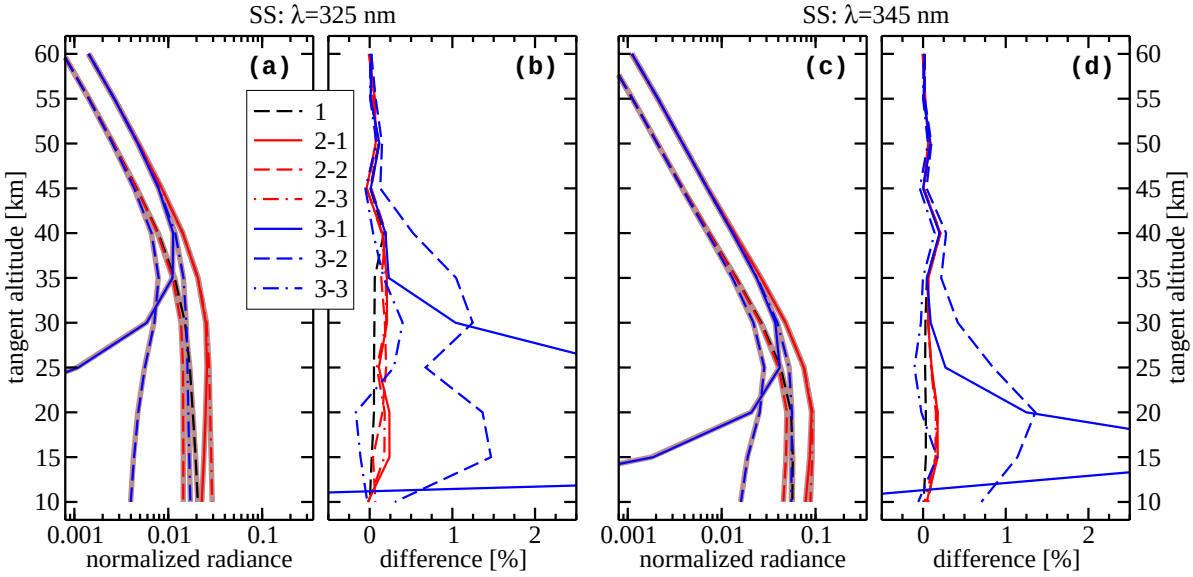

Figure 5.2: *Results of the intercomparison of single scattering contributions. Limb radiances (a,c), modeled by SARTre (colored) and McSCIA (brown), and corresponding percentage deviations (b,d) are presented for $\lambda = 325$ nm (left) and $\lambda = 345$ nm (right). Deviations for case 3-1 reach -5 % to $+15$ % for $\lambda = 325$ nm and ± 5 % at $\lambda = 345$ nm in the lower atmosphere.*

While for optically thin LOS the major part of radiance is contributed by path segments close to the tangent point, the weight is shifted closer to the observer when the LOS becomes optically thick. Although phase function symmetry is still valid, this shifting leads to varying results for symmetric azimuth angles, caused by sun zenith angles – and solar transmission – varying in a different manner along the LOS. This becomes obvious for cases with sun zenith angles of $\mathrm{sza} = 90°$ at the tangent point. At grid points of the observer side of the LOS, the sun is below horizon for case 3-1, "illuminating" these points through limb such that solar transmission becomes very small. Consequently, single scattering source terms are very low, accounting for normalized radiances of $7 \cdot 10^{-6}$ at 345 nm and $4 \cdot 10^{-9}$ at 325 nm only. For cases 3-2 and 3-3 the sun is in or above the horizon for grid points close to the observer. Hence, solar transmission is higher and contributing source terms are larger compared to case 3-1.

Comparing SARTre results to those of McSCIA (see Fig. 5.2(b) and (d)), radiances agree within ±0.5 % at both 325 nm and 345 nm for all tangent altitudes and viewing geometry cases except 3-1 and 3-2. SARTre overestimates radiances of lower tangent heights of case 3-2 by up to 1.5 %. For case 3-1 overestimation reaches up to 5 % at 345 nm and 15 % at 325 nm, while at tangent altitude of 10 km radiance is underestimated by 2 % and 5 %, respectively.

Similar difficulties have been reported e.g. for LIMBTRAN in Loughman et al. (2004). They argue, that the lines of sight for those cases run near the terminator (3-2) or partly in the Earth's shadow (3-1)[2], which makes the modeling more difficult. These cases are primarily characterized by the extremely large path lengths of the solar beam from TOA to the LOS, in particular to the major contributing path segments close to the observer. That means, solar transmission becomes low and varies significantly between subsequent grid points of the LOS. Hence, the large relative deviations are related to accuracy of assumptions made by the path integration technique implemented. The latter presumption is supported by the fact, that a refinement of the grid on which the source terms are evaluated significantly improves the results. A doubling of the number of LOS grid points reduces differences for case 3-1 to −3.5 % to +5.5 % for the SARTre-McSCIA intercomparison at 325 nm. Furthermore, Loughman et al. (2004) state, that "when the layer thickness is reduced by a factor of five [...], the SS divergence is greatly reduced.".

When checking the source term linearity assumption (see 3.1.1), it becomes clear that this breaks down for case 3-1. Although the linearity assumption is met for single scattering albedo ω_0, which is constant within a layer by setup definition, linearity does not apply to solar transmission $\mathcal{T}_\odot$. For case 3-1 the solar path is almost parallel to the LOS and, therefore, $\mathcal{T}_\odot$ varies approximately proportional to $\mathrm{e}^{-\tau}$, where τ is the optical thickness along the LOS. In combination with very small single scattering source terms contributing from points close to the observer, this results in quite large relative deviations (note that absolute differences are rather small in case 3-1). The most extreme version of a case with highly non-linear $\mathcal{T}_\odot$ would be an occultation measurement, to which the linear-in-τ approximation of source terms has to be applied carefully, choosing layer physical thickness appropriately small.

5.3.2 Total Scattering Limb Radiances

After examining the agreement of SARTre and McSCIA for the full spherical part of both models, this subsection focuses on examining the validity of the pseudo-spherical assumption over a range of observing geometries. Total scattering contributions with $TS = SS + MS$ are intercompared, i.e. radiative transfer equation

$$I \;=\; I_{\mathrm{dir}}\,\mathcal{T}_{\mathrm{dir}} \;+\; \int_0^\infty (J_{\mathrm{SS}}(\tau') + J_{\mathrm{MS}}(\tau'))\;\mathrm{e}^{-\tau'}\,\mathrm{d}\tau', \tag{5.4}$$

is evaluated. Single scattering source term J_{SS} corresponds to Eq. (5.3) and J_{MS} is given by

$$J_{\mathrm{MS}} \;=\; \frac{\omega_0}{4\pi} \int_0^{4\pi} P(\mathbf{\Omega}, \mathbf{\Omega'})\, I(\mathbf{\Omega'})\,\mathrm{d}\Omega', \tag{5.5}$$

[2]The statement of the case 3-1 LOS lying partly in the Earth's shadow is inaccurate. It is merely parts of the atmosphere below the LOS lying in the shadow, but not the LOS itself.

with $I(\mathbf{\Omega'})$ being the incident diffuse radiation field, which in SARTre is obtained by solving the RTE in a plane-parallel atmosphere (see subsection 3.1.2). Results of cases with absorbing surface ($r = 0.0$) are presented in Fig. 5.3, while Fig. 5.4 shows results of calculations including a reflecting surface ($r = 1.0$).

Absorbing Surface

TS radiances show a similar behavior with altitude as described in subsection 5.3.1 for SS radiances. In case of an absorbing surface the limb radiances are found to be enhanced between about 1 % to 100 % when taking into account multiple scattering. While SS radiances in the upper atmosphere have been found nearly independent of solar zenith angle (sza), MS contribution is the larger the smaller the sza is. For example, the MS contributions at 325 nm vary between 4 % for sza = 90° and 60 % for sza = 15°. This dependency is found at lower altitudes as well, for which the percentage of MS enhancement is even larger than in the upper atmosphere. Furthermore, relative MS contribution for side illuminated LOS (az = 90°) is larger than in the forward and backward scattering cases, which for optically thin LOS are identical due to Rayleigh scattering symmetry. In the lower atmosphere case 3-1 behaves very different than described before. Since the SS radiances are extremely low (see subsection 5.3.1), MS contribution dominates TS radiances, although absolute MS radiances are only a fraction of those of cases 3-2 and 3-3.

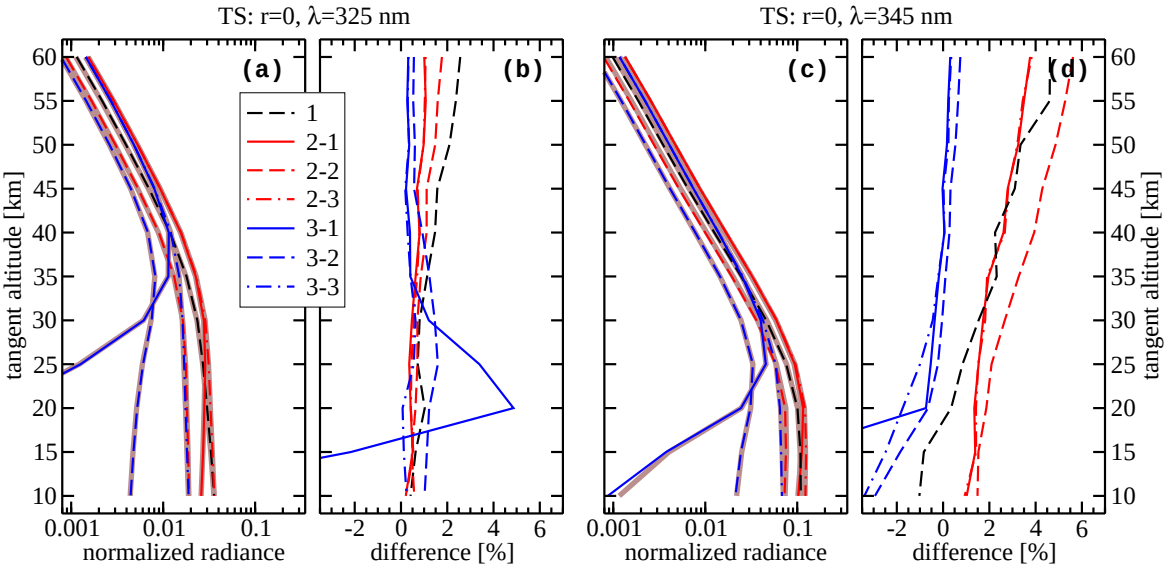

Figure 5.3: *Results of the intercomparison of total scattering contributions in case of absorbing surface. Limb radiances (a,c), modeled by SARTre (colored) and McSCIA (brown), and corresponding percentage deviations (b,d) are presented for $\lambda = 325$ nm (left) and $\lambda = 345$ nm (right).*

Deviations between SARTre and McSCIA toatl scattering radiances are found to be significantly larger than for SS radiances. Except for case 3-1 relative differences are between −0.5 % to +2.5 % at 325 nm and between −3.5 % to +5.5 % at 345 nm, increasing by several percents from 10 to 60 km tangent altitude. This pattern of larger deviations in the upper than in the

lower atmosphere has already been described by Loughman et al. (2004) and Griffioen and Oikarinen (2000) and seems typical for pseudo- or approximate spherical models. Griffioen and Oikarinen (2000) suppose this to be caused by photons more readily escaping a spherical than a plane-parallel atmosphere, which becomes more apparent toward the top of the atmosphere, and suggest it to be an effect of missing limb darkening in plane-parallel models.

Reflecting Surface

In case of a fully reflecting surface, mostly similar results compared to the non-reflecting surface cases are revealed. However, TS radiances are significantly enhanced by surface effects for all observation geometries. Similar to atmospheric scattering, surface reflection effects are the larger, the smaller the solar zenith angle is. With large zenith angles, less sun light is able to penetrate to and be scattered off the surface. Thus, MS contribution including surface reflection is largest for case 1, where it reaches up to 200 % at 345 nm and low tangent altitudes.

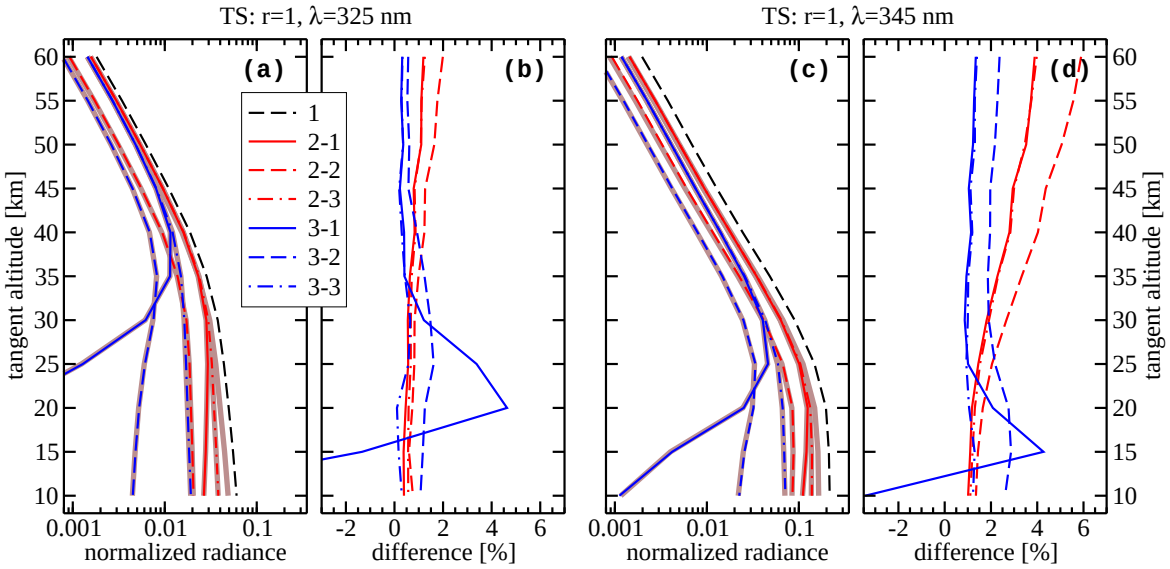

Figure 5.4: *Results of the intercomparison of total scattering contributions in case of absorbing surface. Limb radiances (a,c), modeled by SARTre (colored) and McSCIA (brown), and corresponding percentage deviations (b,d) are presented for λ = 325 nm (left) and λ = 345 nm (right). Case 1 deviations, not shown in the difference plot, are ≈ 30 % (325 nm) to 40 % (345 nm).*

SARTre and McSCIA diverge by the same magnitudes as for absorbing surface except for case 1, where differences of up to +40 % of TS radiances occur. Although a coincidence of high sun and totally reflecting surface is rarely found in Earth remote sensing, due to the large MS contributions case 1 is indeed a crucial case for testing the validity of the pseudo-spherical assumption. Effects of reduced sphericity in multiple scattering modeling, that probably vanish in relation to SS radiances for cases of large sza, obviously become noticeable. Besides, a strong contribution from the surface is a further challenge to the pseudo-spherical assumption, such that deviations could be expected to increase comparing to absorbing surface cases. However, while the results for absorbing surface agree very well with the findings of Loughman et al. (2004),

approximate models there have been found to overestimate TS radiances in case of reflecting surface by 10 % only. This indicates, that deviations between SARTre and McSCIA are not solely due to different geometrical approaches, but that the implementation of reflecting surfaces is not correct in either SARTre or McSCIA.

Concerning that issue, a simple test case of an 8-layer conservative Rayleigh scattering atmosphere, bounded by a fully reflecting surface, has been set up to assure a correct surface reflection implementation in SARTre. Upwelling radiances, modeled by SARTre for a quasi plane-parallel atmosphere ($R = 6.3 \cdot 10^6$ km) of all combinations of 13 observer viewing angles, 13 solar zenith angles and 7 relative azimuth angles, covering the complete upper hemisphere, have been compared to results from DISORT and STORM. Quasi plane-parallel SARTre calculations agreed within ± 1 % to DISORT radiances. In comparison to radiances calculated by the independent vector RT model STORM, deviations of $< \pm 5$ % have been observed, which can be explained by polarization effects.

5.4 Summary

This chapter has dealt with the verification of solar radiative transfer in a spherical atmosphere, that is illuminated by a beam source. Verification has been done by an intercomparison to the Monte Carlo model McSCIA. Emphasis was placed on testing the full spherical implementation of single scattering as well as the validity of the pseudo-spherical assumption over a wide range of observation geometries. Other issues, e.g. line-by-line calculation of molecular absorption cross sections and parameterization of path optical depth along the line of sight, remained unchecked due to the input setup.

In general, the single scattering contributions of SARTre and McSCIA agreed within some tenth of a percent. Caution is advised in cases, where the linearity assumption to the source terms breaks down. In contrast to the breakdown discussed in section 4.6, which occurs due to the non-linearity of the single scattering albedo within a path segment, here the transmission of sun light is prone to not satisfy this assumption. In particular, problems may occur when the path of the solar beam from top-of-atmosphere to the scattering point becomes optically very thick. Currently, the user is responsible to assure source term linearity between given altitude profile grid points. For a future version the implementation of a procedure, that supervises and assures the linearity criterium automatically, is recommended.

When considering multiple scattering, which significantly enhances observed limb radiances, in particular when the solar zenith angle is small, differences are found to be of a magnitude of several percent. SARTre performs well for $\lambda = 325$ nm, where ozone absorption is significant and deviations do not exceed 2.5 %, as well as for the lower tangent altitudes in the conservative scattering atmosphere at $\lambda = 345$ nm for both absorbing and fully reflecting surfaces. The pseudo-spherical approach reaches its limits when radiances of high tangent altitudes in strongly scattering atmospheres are modeled. Then, deviations of > 5 % occur.

Large disagreement between SARTre and McSCIA is observed for small solar zenith angles in combination with a reflecting surface. Currently, reasons remain unclear, but an inconsistent surface implementation in McSCIA or SARTre is likely. Comparisons to DISORT and the independent plane-parallel model STORM did not show significant deviations to SARTre in case of reflecting surface.

Furthermore, difficulties are encountered at low tangent altitudes with the sun in forward scattering direction at or below the horizon. Then, atmospheric path lengths of the solar beam are very large and the single scattering contribution becomes extremely low. Similar effects had already been observed in Loughman et al. (2004) for full spherical non-Monte-Carlo models as well as for approximate spherical models.

Concerning calculation time, SARTre is not competitive yet, when modeling radiative transfer in an atmosphere illuminated by a beam source. Currently the incident radiance field for the multiple scattering term is solved at each grid point along the LOS, which generally is not necessary. Radiance fields may be derived for a small set of solar zenith angles and interpolated for other angles without significant loss of accuracy, since solar angles do not change rapidly along the line of sight. Furthermore, computation time increases linearly with the number of layers and with the square of the number of streams used when solving the incident diffuse radiation field. At present, the number of layers is controlled by the altitude grid of input atmospheric profiles, while the number of streams is an input parameter defined by the user. The number of computational layers, in particular, is a parameter that presumably could be optimized without big efforts in most cases. Finally, no computational optimization of radiance calculations for multiple tangent altitudes has been done yet.